Soliton emission at a phase-mismatch boundary in a quadratic nonlinear film waveguide

Fabio Baronio* and Costantino De Angelis

Istituto Nazionale per la Fisica della Materia, Università di Brescia, via Branze 38, 25123 Brescia, Italy

Paul-Henri Pioger, Vincent Couderc, and Alain Barthélémy

Faculté des Sciences, Institut de Recherches en Communications Optiques et Microondes, 123 Avenue A. Thomas, 87060 Limoges, France

Yoohong Min, Victor Quiring, and Wolfgang Sohler

Angewandte Physik, Universität Paderborn, 33095 Paderborn, Germany

Received April 7, 2003

We report the experimental demonstration of spatial nonlinear beam displacement caused by an interface between periodically modulated and uniform quadratic nonlinearity. We observe intensity- and phase-mismatch-dependent spatial beam displacement at 1548 nm in lithium niobate waveguides. The device has the potential to provide a soliton-emission-based, ultrafast all-optical switch. © 2003 Optical Society of America

OCIS codes: 190.4420, 070.4340, 060.5530.

The propagation of light in the vicinity of an interface between two nonlinear dielectrics has been widely studied in the past four decades following the milestone research of Bloembergen and Pershan[1] and of Kaplan.[2] Nonlinear transverse field effects at the interface between second-order[3,4] and third-order[5,6] nonlinear dielectrics have been predicted. However, few experimental results are available.[7,8] In the framework of quadratically nonlinear media, quasi-phase matching can be used in engineering nonlinear structures. This technique opens a whole range of new possibilities that have become experimentally feasible with reproducible fabrication of periodically poled lithium niobate (PPLN). Engineered PPLN patterns show promise for use in soliton systems. Soliton reflection, tunneling, resonant trapping, and emission in engineered structures have been predicted.[9,10]

In this Letter we describe electromagnetic nonlinear type I interaction of a fundamental wave [(FF) at 1548 nm] and a second-harmonic wave [(SH) at 774 nm]. We investigate spatial propagation of beams in titanium-indiffused lithium niobate slab waveguides across an interface between a periodically poled and a homogeneous lithium niobate region, with a FF only in the input (see Fig. 1). In this situation, the parametric wave-mixing interaction is highly efficient in the region with the domain grating, whereas in the homogeneous waveguide the mixing efficiency is negligible. For a given input power, because of the interface between two nonlinear regions, the beams switch into the domain grating (soliton emission). We performed an experimental demonstration of a nonlinear spatial transverse deflection of a soliton beam. Intensity- and phase-mismatch-dependent spatial displacement was measured.

The experiments were performed with a 58-mm-long Ti:$LiNbO_3$ Z-cut planar waveguide. A microdomain structure of 16.92-μm periodicity was generated after waveguide fabrication by electric field assisted poling in one part of the waveguide only. The planar waveguide had a transition Ti:PPLN/Ti:$LiNbO_3$ between periodically poled and unpoled regions. The sample was inserted into a temperature-stabilized oven to permit operation at elevated temperatures ($T = 120-160$ °C); in this way, photorefractive effects (optical damage) could be minimized and temperature tuning of the phase-matching conditions became possible. An all-fiber laser system was used as the source of 4-ps pulses (FWHM) at 1548 nm (FF) of 1.7-nm spectral bandwidth and of a peak power of a few kilowatts at a 20-MHz repetition rate. The laser beam was shaped in a highly elliptical spot, nearly Gaussian in profile, with $w_{0x} = 60$ μm (FWHM) along the waveguide plane and $w_{0y} = 3.9$ μm along the perpendicular direction. We recorded the spatial beam profiles by scanning a magnified image of the pattern with a photodiode.

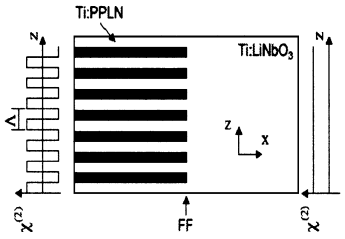

Fig. 1. Schematic of the nonlinear nonuniform geometry: a homogeneous Ti:$LiNbO_3$ region interfaced to a Ti:PPLN region.

0146-9592/03/232348-03$15.00/0

We model electric fields E_1 and E_2, at ω_0 (FF) and $2\omega_0$ (SH), respectively, propagating in the z direction, as

$$E_1(x,y,z,t) = \tfrac{1}{2}\{W(y)w(x,z,t) \times \exp\{-j[\beta(\omega_0)z + \omega_0 t]\} + \text{c.c.}\},$$

$$E_2(x,y,z,t) = \tfrac{1}{2}\{V(y)v(x,z,t) \times \exp\{-j[\beta(2\omega_0)z + 2\omega_0 t]\} + \text{c.c.}\},$$

where $W(y)$ and $V(y)$ are the mode profiles and $w(x,z,t)$ and $v(x,z,t)$ are the slowly varying envelopes. Envelopes $w(x,z,t)$ and $v(x,z,t)$ obey the nonlinear coupled equations[11]

$$j\frac{\partial w}{\partial z} - j\beta_{\omega_0}{}'\frac{\partial w}{\partial t} - \frac{\beta_{\omega_0}{}''}{2}\frac{\partial^2 w}{\partial t^2} + \frac{1}{2\beta_{\omega_0}}\frac{\partial^2 w}{\partial x^2} + \frac{\chi^{(2)}\omega_0}{2cn_{\omega_0}}\frac{\int V|W|^2\,dy}{\int |W|^2\,dy}\,vw^*\exp(-j\Delta kz) = 0,$$

$$j\frac{\partial v}{\partial z} - j\beta_{2\omega_0}{}'\frac{\partial v}{\partial t} - \frac{\beta_{2\omega_0}{}''}{2}\frac{\partial^2 v}{\partial t^2} + \frac{1}{2\beta_{2\omega_0}}\frac{\partial^2 v}{\partial x^2} + \frac{\chi^{(2)}\omega_0}{2cn_{2\omega_0}}\frac{\int V|W|^2\,dy}{\int |V|^2\,dy}\,w^2\exp(j\Delta kz) = 0, \quad (1)$$

where β represents the propagation constant, β' is the inverse group velocity, β'' is the inverse group-velocity dispersion, n is the refractive index, $\Delta k = 2\beta_{\omega_0} - \beta_{2\omega_0}$ is the phase mismatch, and $\chi^{(2)}$ is the nonlinear coefficient. In the unpoled region, $\chi^{(2)} = \chi^{(2)}_{z'z'z'}$; in the PPLN region, nonlinear term $\chi^{(2)}(z)$ consists of domains of nonlinear coefficient $\pm\chi^{(2)}_{z'z'z'}$ with sign changes that occur with periodicity $\Lambda/2$. In the PPLN region the behavior of the wave-mixing interaction is similar to that of a conventionally phase-matched interaction but with an effective mismatch Δk_{eff} shifted by an amount $K_s = 2\pi/\Lambda$ with respect to Δk and with an effective nonlinear coefficient $\chi^{(2)}(z) = 2/\pi\chi^{(2)}_{z'z'z'}$. Under this assumption

$$\Delta k(z) = \begin{cases} 2\beta_{\omega_0} - \beta_{2\omega_0} + 2\pi/\Lambda & x \le 0 \\ 2\beta_{\omega_0} - \beta_{2\omega_0} & x > 0 \end{cases},$$

$$\chi^{(2)}(x) = \begin{cases} 2/\pi\chi^{(2)}_{z'z'z'} & x \le 0 \\ \chi^{(2)}_{z'z'z'} & x > 0 \end{cases}. \quad (2)$$

We employed a finite-difference vectorial mode solver to determine the linear propagation properties of the slab waveguide. In the case at hand, crystal length L corresponds to 5.6 times the FF diffraction length and to 5.2 times the walk-off length between the FF and the SH; the dispersive terms can be neglected. Finally, using a finite-difference beam propagation technique, we solved the nonlinear coupled equations [Eqs. (1)].

We carried out experiments and numerical simulations by launching the FF input beam parallel to the nonlinear interface, varying the spatial input displacement, the input pulse power, and the phase-mismatch conditions by varying the temperature of the sample, keeping fixed the temporal and spatial widths of the injected FF pulse. Far from the interface, in the PPLN region, spatial self-trapping could be induced even if the pump pulse's duration was shorter than the group-delay mismatch between FF and SH components.[12] In the quasi-linear regime the output beam profile had a width $w_{0x} = 320\ \mu$m that corresponded to the diffracted input beam ($w_{0x} = 60\ \mu$m) after 58 mm of propagation along the waveguide. When the incident intensity was increased, at large enough positive phase-mismatch values ($\Delta kL > 9\pi$) the nonlinear self-focusing balanced the effect of diffraction, causing the formation of a spatial soliton. In Fig. 2, typical numerical and experimental results are shown.

We then launched the FF input beam in the PPLN region, close to the interface between the PPLN region and the unpoled region. Again, in the quasi-linear regime, at low intensity, the beam broadened because of diffraction inside the crystal. Increasing the incident intensity, at large enough phase mismatch in the PPLN region ($\Delta kL > 9\pi$) we succeeded in exciting a spatial soliton, and we observed its spatial shift. In Fig. 3, typical numerical and experimental results are shown. In essence, the beam experienced effective spatial acceleration and consequently spatial velocity in the transverse dimension (x) toward the region where the nonlinear interaction is more efficient. This phenomenon (soliton emission) can be attributed to the existence of a nonlinear repulsive potential well induced by the effective nonlinear interface. The intensity of the repulsive potential is inversely proportional to the separation distance between the input beam and the transition. A distance exceeding 30 μm was sufficient to suppress any spatial shifting

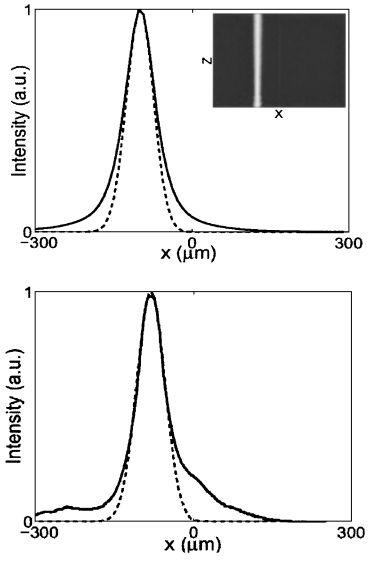

Fig. 2. Propagation in the Ti:PPLN region. Input (dashed curve) and output (continuous curve) FF spatial profile in the soliton regime. Top, numerical simulations; bottom, experimental data. Inset, the numerical evolution of the soliton in the (x,z) plane. $I = 160$ MW/cm^2 and $\Delta kL = 15\pi$ ($T = 147\,^\circ$C).

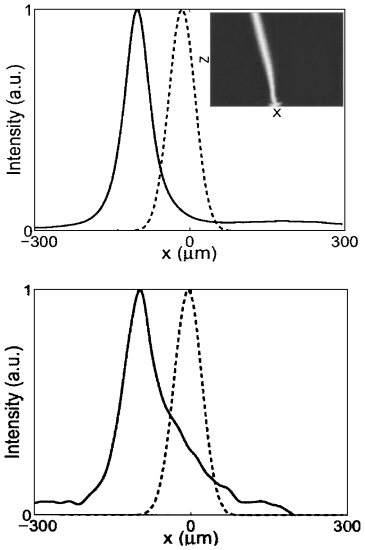

Fig. 3. Propagation close to the interface. Input (dashed curve) and output (continuous curve) FF spatial profile in the soliton regime. Top, numerical simulations, bottom, experimental data. Inset, the numerical evolution of the soliton in the (x, z) plane. $I = 800\ \mathrm{MW/cm^2}$, $\Delta kL = 15\pi$ in the Ti:PPLN region; $\Delta kL \approx -6000\pi$ in the unpoled region ($T = 147\,^{\circ}\mathrm{C}$).

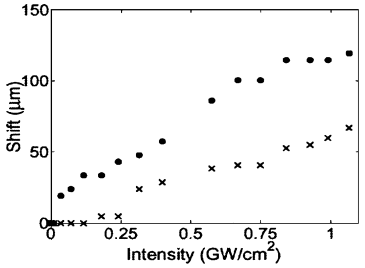

Fig. 4. Measured FF spatial shift on the output face of the crystal versus intensity for two temperatures [147 °C ($\Delta kL = 15\pi$), top trace; 127 °C ($\Delta kL = 37\pi$), bottom trace].

of the trapped beam. The soliton emission phenomenon is intensity and phase-mismatch dependent. Experimental results concerning the spatial shift of the FF output beam versus intensity and for different phase-mismatch conditions are shown in Fig. 4. Because the pulse duration (~4 ps) is significantly shorter than the group-delay mismatch between FF and SH components, spatial soliton propagation can be induced only for large positive phase mismatch. The use of longer pulses should permit emission to be obtained at the phase-matching condition and should increase the spatial soliton deflection.

In conclusion, we have described spatial soliton emission that is due to spatially varying effective nonlinearity in nonuniform lithium niobate waveguides at 1548 nm. We observed the spatial displacement of the trapped beam versus the input intensity and versus the phase mismatch. The intensity and wavelength dependence of the soliton emission phenomenon portends new applications for ultrafast all-optical devices.

This research was performed in the framework of European project ROSA (Information Society Technologies/Future and Emerging Technologies) supported by the European Commission. C. De Angelis's e-mail address is deangeli@ing.unibs.it.

*Also with the Istituto Nazionale per la Fisica della Materia, Dipartimento di Ingegneria dell'Informazione, Università di Padova, Via Gradenigo 6/a, 35131 Padua, Italy.

References

1. N. Bloembergen and P. S. Pershan, Phys. Rev. **128,** 606 (1962).
2. A. E. Kaplan, Sov. Phys. JETP **45,** 896 (1977).
3. A. D. Capobianco, C. De Angelis, A. Laureti Palma, and G. Nalesso, J. Opt. Soc. Am. B **14,** 1956 (1997).
4. I. V. Shadrivov and A. A. Zharov, J. Opt. Soc. Am. B **19,** 596 (2002).
5. A. B. Aceves, J. V. Moloney, and A. C. Newell, Phys. Rev. A **39,** 1809 (1989).
6. Y. S. Kivshar, A. M. Kosevich, and O. A. Chubykalo, Phys. Rev. A **41,** 1677 (1990).
7. P. Dumais, A. Villeneuve, A. Saher-Helm, J. S. Aitchison, L. Friedrich, R. A. Fuerst, and G. I. Stegeman, Opt. Lett. **25,** 1282 (2000).
8. E. A. Mendez, R. R. Laguna, J. G. A. Cervantes, M. T. Cisneros, J. A. A. Lucio, J. C. P. Ortega, E. A. Kuzin, J. J. S. Mondragón, and V. Vysloukh, Opt. Commun. **193,** 267 (2001).
9. C. Balslev Clausen and L. Torner, Phys. Rev. Lett. **81,** 790 (1998).
10. F. Baronio and C. De Angelis, IEEE J. Quantum Electron. **38,** 1309 (2002).
11. G. I. Stegeman, D. J. Hagan, and L. Torner, Opt. Quantum Electron. **28,** 1691 (1996).
12. P. Pioger, V. Couderc, L. Lefort, A. Barthelemy, F. Baronio, C. De Angelis, Y. Min, V. Quiring, and W. Sohler, Opt. Lett. **27,** 2182 (2002).